

THE OFFICIAL MAGAZINE OF THE OCEANOGRAPHY SOCIETY

# Oceanography

## CITATION

Klotz, P., I.R. Schloss, and D. Dumont. 2018. Effects of a chronic oil spill on the planktonic system in San Jorge Gulf, Argentina: A one-vertical-dimension modeling approach. *Oceanography* 31(4):81–91, <https://doi.org/10.5670/oceanog.2018.413>.

## DOI

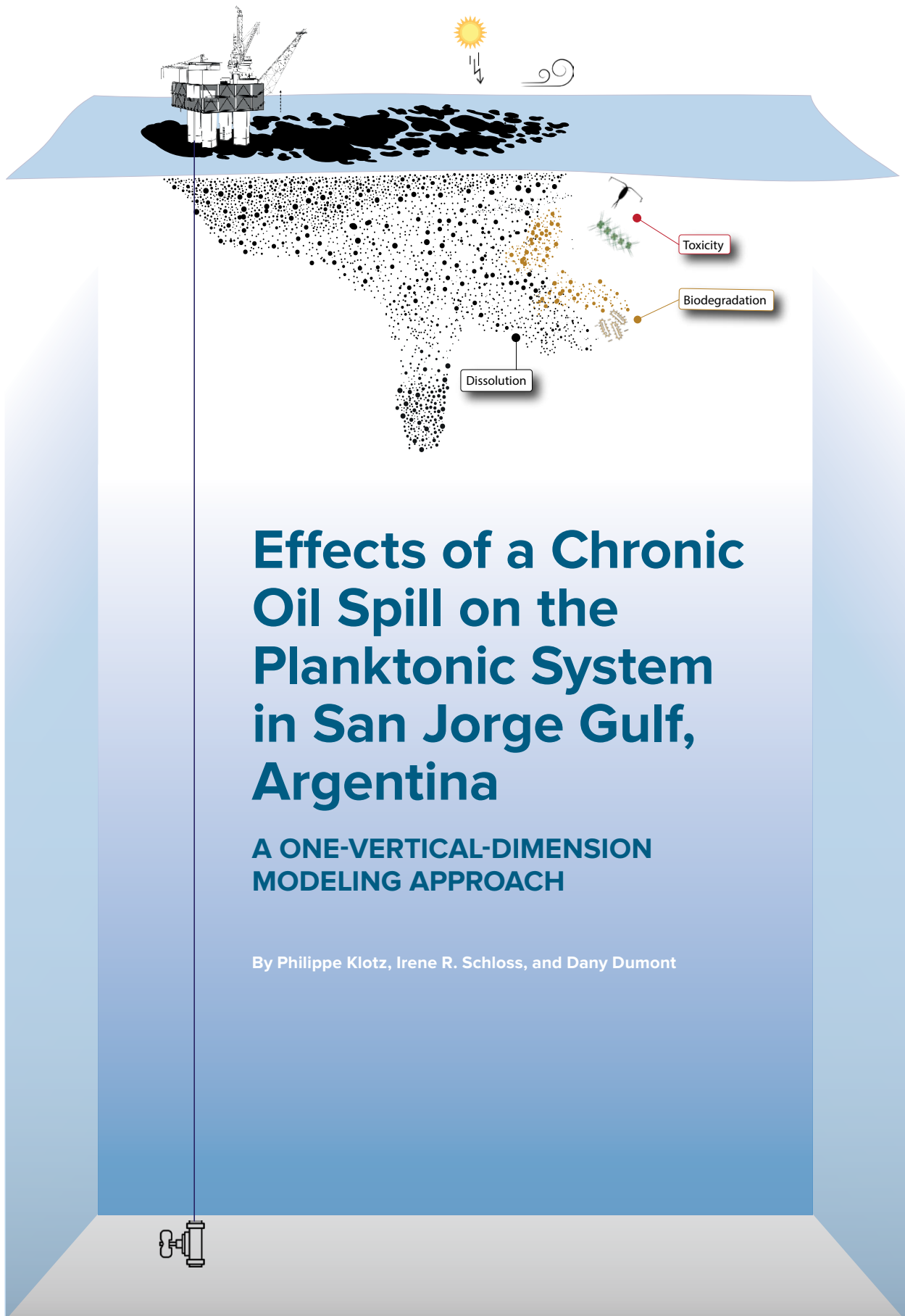
<https://doi.org/10.5670/oceanog.2018.413>

## PERMISSIONS

*Oceanography* (ISSN 1042-8275) is published by The Oceanography Society, 1 Research Court, Suite 450, Rockville, MD 20850 USA. ©2018 The Oceanography Society, Inc. Permission is granted for individuals to read, download, copy, distribute, print, search, and link to the full texts of *Oceanography* articles. Figures, tables, and short quotes from the magazine may be republished in scientific books and journals, on websites, and in PhD dissertations at no charge, but the materials must be cited appropriately (e.g., authors, *Oceanography*, volume number, issue number, page number[s], figure number[s], and DOI for the article).

Republication, systemic reproduction, or collective redistribution of any material in *Oceanography* is permitted only with the approval of The Oceanography Society. Please contact Jennifer Ramarui at [info@tos.org](mailto:info@tos.org).

Permission is granted to authors to post their final pdfs, provided by *Oceanography*, on their personal or institutional websites, to deposit those files in their institutional archives, and to share the pdfs on open-access research sharing sites such as ResearchGate and Academia.edu.



# Effects of a Chronic Oil Spill on the Planktonic System in San Jorge Gulf, Argentina

**A ONE-VERTICAL-DIMENSION MODELING APPROACH**

By Philippe Klotz, Irene R. Schloss, and Dany Dumont

**ABSTRACT.** Known for its high biological productivity, San Jorge Gulf (SJG) in Argentinian Patagonia is also an area of oil exploitation. To understand the dynamics of the SJG plankton ecosystem under several scenarios of potential hydrocarbon (HC) contamination, we present an 11-compartment biogeochemical model coupled to a turbulence model. In the coupled model, we parameterize the main physical and biological processes related to HC contamination, such as biodegradation, growth, and mortality of phyto-, zoo-, and bacterioplankton. Planktonic responses to several levels of HC contamination are studied for two physically contrasting SJG environments, a tidally well-mixed water column and a stratified water column. Results show increasing phyto- and bacterioplankton biomass with increasing HC concentration, which in turn produces more detritus. Zooplankton communities seem to respond differently depending on HC concentration, with major indirect changes occurring in the different size classes. Effects of HC contamination on biological compartments are stronger in the stratified than in the well-mixed environment.

## INTRODUCTION

Since the beginning of the twentieth century, along the Argentinian coast, particularly within San Jorge Gulf (SJG), oil production has been the main economic driver, accounting for nearly half of total oil production in the country (Ministerio de Energía y Minería, 2016). Offshore exploration and extraction of this resource pose risks to the gulf's marine ecosystem. Thus, it is essential to understand the physical and biological dynamics of this coastal system. The SJG is exposed to strong sustained westerly winds throughout the year as well as strong semi-diurnal tidal currents, and is characterized by a counterclockwise circulation (Glorioso and Simpson, 1994; Glorioso and Flather, 1995; Palma et al., 2004). In the shallow ( $\leq 80$  m) southeastern area of the SJG, the bottom friction of strong tidal currents results in significant turbulent mixing (Glorioso and Flather, 1995) that creates a permanent, mainly tidally induced, frontal zone (Glorioso and Flather, 1997; Palma et al., 2004; Flores-Melo et al., 2018, in this issue) This is confirmed by sharp horizontal gradients evident in satellite observations of temperature and chlorophyll-*a* (Chl*a*) concentrations in the region (Acha et al., 2004; Rivas et al., 2006; Glembocki et al., 2015). Areas of high biological productivity are often associated with high horizontal density gradients, where turbulence plays a role not only in the availability of nutrients in the euphotic zone but also in

the distribution of phytoplankton biomass (Flores-Melo et al., 2018, in this issue).

It is difficult to study and quantify the effects of hydrocarbons (HC) on planktonic assemblages in situ. Micro- and mesocosm experiments provide ways to target the direct effects of contamination on plankton by controlling experimental conditions such as nutrient concentration, temperature, and light intensity, which affect the growth, mortality, and distribution of organisms. However, because coupled biological-physical processes are nonlinear, the influence of physical factors cannot be accounted for in these kinds of studies.

Dissolved HC, especially polycyclic aromatic hydrocarbons (PAHs), contribute up to 60% of the total oil composition (Fingas, 2016) and have the most negative effect on marine organisms. The hydrophobic nature of these compounds and their bioavailability once they are dissolved in the marine environment favor their adsorption by marine organisms. As a result, mortality increases through simple toxicity or by reduction of the organism's physiological activity (Anderson et al., 1974).

In contrast, specific strains of bacterioplankton contribute to one of the most persistent disaggregation processes found during an HC contamination event: biodegradation (Beazley et al., 2012). Since the early twentieth century, study of the bacteria genome has made it possible to isolate more than 70 genera capable

of degrading HC (Hassanshahian and Cappello, 2013). In the marine environment, bacterioplankton exhibit significant changes in community structure and biomass following oil spills (Hazen et al., 2010; Dubinsky et al., 2013). These marine bacteria, known as obligate HC-degrading bacteria (OHCB; Yakimov et al., 2007), are ubiquitous at very low concentrations in the water column and are characterized by high substrate specificity.

In order to assimilate HC through fast growth rates, bacterioplankton depend on the concentration of dissolved oxygen and nutrients in the water column (Valentine et al., 2012; King et al., 2015). For example, phosphorus- and nitrogen-based compounds seem to act as regulators of biodegradation processes (Atlas and Bartha, 1972; Horowitz and Atlas, 1977; Atlas, 1981), thus limiting or promoting HC incorporation into pelagic carbon biomass (Shiller and Joung, 2012). However, the scarcity of information concerning the limiting nutrient forms and their related consumption makes it difficult to estimate precise biodegradation rates associated with HC spreading in seawater.

Of all the microorganism classes, phytoplankton display the highest variability in their response to HC contamination. From an ecotoxicological perspective, some phytoplankton groups appear to be more affected than others at equivalent concentrations. This is the case for diatoms, whose growth may sharply decrease (Hsiao, 1976; Nayar et al., 2005) because their siliceous walls significantly adsorb and accumulate PAHs (Siron et al., 1996; Sargian et al., 2007). However, other results show phytoplankton growth is stimulated at low concentrations of the dissolved HC fraction (Gordon and Prouse, 1973; Dunstan et al., 1975; Hsiao et al., 1978; González et al., 2013). The mechanisms associated with an increase in photosynthetic activity are poorly understood and lead to several hypotheses. For example, Baker (1971) and Cabioch et al. (1981) suggest

that extra nutrient uptake by phytoplankton is a result of the degradation of dead organisms by HC toxicity.

HC appears to affect all major zooplankton groups, but effects differ depending on species and HC concentrations. Almeda et al. (2013) observed 96% copepod mortality after 16 hours of exposure to PAH concentrations of 100  $\mu\text{L}^{-1}$ . They also calculated a mean lethal concentration ( $\text{LC}_{50}$ ) of 31.4  $\mu\text{L}^{-1}$ .

Modeling allows simulation of pelagic system biogeochemical dynamics in realistic physical settings as well as simulation of the effects of contamination on plankton. The General Ocean Turbulence Model (GOTM) developed by Burchard et al. (2006) is a one-dimensional model of turbulence in the vertical dimension that can be coupled to a biogeochemical model of the nitrate-phytoplankton-zooplankton type (i.e., following Fasham et al., 1990). The coupled model can simulate the annual evolution of the mixing depth and include the processes related to the microbial loop. The effect of contaminants on the biological compartments can be further parameterized, allowing for a complete physical and biological interpretation of the effects of pollutants on plankton. Previous studies have simulated the behavior of HC in the marine environment (Reed et al., 1999), but only a few models have measured their impacts on the biogeochemical dynamics of the planktonic system (Gin et al., 2001; Valentine et al., 2012; González et al., 2013).

In this study, we combine data from the scientific literature and from the 2014 PROMESse mission in the SJG (Flores-Melo et al., 2018, and Latorre et al., 2018, both in this issue) to simulate an offshore oil spill event. Using a one-dimensional biogeochemical-physical modeling approach, we evaluate the response of plankton to chronic HC contamination in a turbulent environment. Two mixing regimes typical of the southeastern frontal region of the SJG are compared: a seasonally stratified zone and a shallower, tidally well-mixed zone.

## MODEL DESCRIPTION

### Physical Model and Configuration

We used the GOTM coupled to a biogeochemical model to solve the advection-diffusion problem in the vertical dimension, assuming that state variables are horizontally homogeneous and that both mean and turbulent transport are driven by wind, buoyancy fluxes, and shear production. Horizontal advection is not taken into account. A detailed configuration of the two hydrodynamically contrasting experiments (stratified and well-mixed) can be found in the online supplementary materials.

### Biogeochemical Model and Configuration

The biogeochemical model is composed of 11 compartments (see Figure 1), with a nitrate-phytoplankton-zooplankton-detritus (NPZD)-based structure con-

nected to a microbial loop that reproduces nitrogen recycling from labile dissolved organic nitrogen (LDON) to ammonium ( $\text{NH}_4^+$ ). Because nitrogen is the limiting element in most marine ecosystems (Howarth, 1988), understanding its dynamics is an essential prerequisite to describing the carbon cycle (Fasham et al., 1990). Each biogeochemical variable is then expressed in nitrogen concentrations ( $\text{mmol N m}^{-3}$ ).

The model's biological super-compartments combine two compartments each of bacteria, phytoplankton, and zooplankton. In the bacterial super-compartment, BAC1 represents the bacterioplankton involved in the natural microbial loop that are only responsible for nitrogen recycling of detritus from LDON to ammonium. BAC2 represents the hydrocarbon-degrading or "OHCB" strains that are

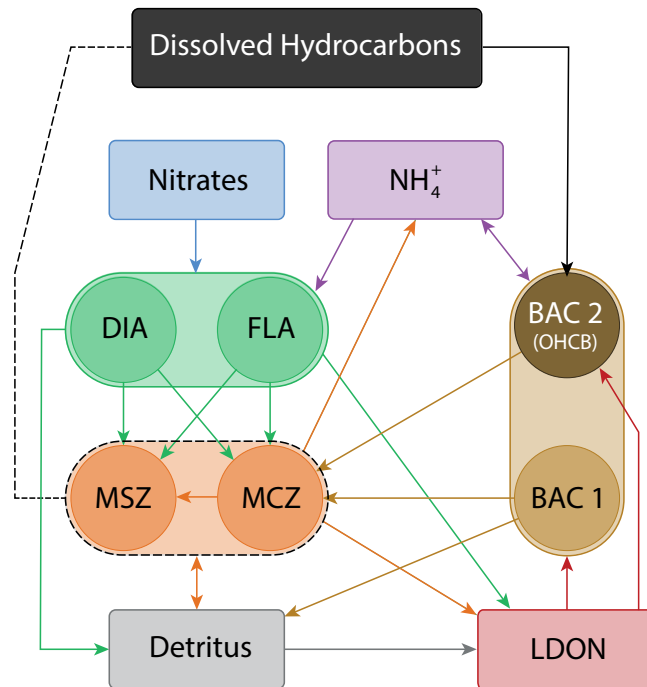


**FIGURE 1.** The general structure of the biogeochemical model is composed of 11 compartments: dissolved hydrocarbons, nitrates, ammonium ( $\text{NH}_4^+$ ), diatoms (DIA), flagellates (FLA), microzooplankton (MCZ), mesozooplankton (MSZ), bacteria community (BAC1), obligate hydrocarbon degrading bacteria (BAC2 [OHCB]), labile dissolved organic nitrogen (LDON), and detritus. Dashed lines illustrate the direct effects of hydrocarbons on biological compartments. Each arrow represents a flux and each compartment a concentration in  $\text{mmol N m}^{-3}$ . Three super-compartments combine the two bacterial compartments (brown), the two phytoplankton compartments (green), and the two zooplankton components (orange).

found in high concentrations in oil-contaminated waters (see later section on Biodegradation).

Two phytoplankton groups, diatoms and flagellates, constitute the main size classes of organisms found in the SJG (Latorre et al., 2018, in this issue). In order to understand the indirect effects of HC on this super-compartment, both groups were parameterized with the same growth rates, initial concentrations, and settling velocities. Differences between diatoms (DIA) and flagellates (FLA) were only prescribed for mortality, zooplankton grazing preferences, natural sinking velocities, and transformation into detritus. An exudation factor reproduces the transfer of nitrogen to LDON. Given the high variability of HC effects on phytoplankton, no direct effect was parameterized and only the indirect effects were characterized.

Micro- (MCZ) and mesozooplankton

(MSZ) represent two zooplankton classes in the model. Microzooplankton graze on diatoms, flagellates, detritus, and bacteria, and mesozooplankton graze on diatoms, flagellates, detritus, and microzooplankton. Zooplankton loss by exudation, natural mortality, and mortality by HC toxicity are the three sink terms leading to fluxes toward the ammonium, LDON, and detritus compartments (Table 1, Equations 1.3 and 1.4). Parameterization of nitrogen dynamics, which concern nitrate and ammonium, is described in supplementary materials.

### Parameterization of HC Effects

To simulate the presence of HC in the GOTM, we considered a new variable: the portion of HC dissolved in seawater that results from weathering processes. As the literature suggests, the dissolved portion, also called the “water accommodated

fraction,” is considered to be the most toxic HC state for marine biota (Anderson et al., 1974). Only the zooplankton super-compartment is parameterized by direct effects related to HC toxicity (see later section on Effects of HC on Zooplankton Mortality). Therefore, effects on phytoplankton dynamics after HC contamination are only indirect effects.

### Biodegradation

Biodegradation of oil spill compounds involves a large number of specific organisms and biochemical processes. Thus, quantifying the transfer of carbon to the planktonic food web remains challenging. After several model runs, we chose the processes to integrate into the GOTM structure. Because the compounds in the extracted oil are composed of  $\leq 1\%$  nitrogen (Musser and Kilpatric, 1998; Fingas, 2016; Petroleum HPV Testing Group,

**TABLE 1.** Biogeochemical equations and parameters involved in the biodegradation process (Equations 1.1 and 1.2) and the mortality of micro- and mesozooplankton by hydrocarbon toxicity (Equations 1.3, 1.4, 1.5, and 1.6). Biogeochemical fluxes from the output (o) toward the input (i) compartment follow the nomenclature:  $C_{o,i}$ .

| Equation  | Parameter        | Definition   | Unit                   |
|---|------------------|--|------------------------|
| $C_{11,6} = vb_2 \min_{hi}(C_6 + C_b^{min})$ Hydrocarbon uptake by “OHCB” (1.1)   | $C_{11}$         | Hydrocarbon concentration  | mmol N m <sup>-3</sup> |
|   | $C_6$            | Obligate HC-degrading bacteria (OHCB) bacterial concentration            | mmol N m <sup>-3</sup> |
|   | $C_9$            | Labile Dissolved Organic Nitrogen concentration (LDON)                   | mmol N m <sup>-3</sup> |
| $\min_{hi} = \min\left(\frac{C_{HC}}{K_{10} + C_{11}}; \frac{C_9}{K_4 + C_9}\right)$ Minimal HC to LDON uptake ratio for “OHCB” Bacteria (1.2)  | $vb_2$           | Maximal uptake rate of OHCB  | day <sup>-1</sup>      |
|   | $K_4$            | Half saturation constant of traditional bacteria uptake                  | –                      |
|   | $K_{10}$         | Half saturation constant of OHCB uptake                                  | –                      |
| $C_{3,7} = (1 - \beta)(g_2^{max} \rho_{18} C_3^2 Fac_2) + (1 - \varepsilon - \delta) \mu_{21}^{HC} \frac{(C_3 + C_z^{min})}{K_6 + (C_3 + C_z^{min})}$ Degradation of microzooplankton in detritus (1.3) | $C_3$            | Microzooplankton concentration   | mmol N m <sup>-3</sup> |
|   | $C_4$            | Mesozooplankton concentration  | mmol N m <sup>-3</sup> |
|   | $C_7$            | Detritus concentration   | mmol N m <sup>-3</sup> |
|   | $C_{11}$         | Hydrocarbon concentration  | mmol N m <sup>-3</sup> |
| $C_{4,7} = (1 - \varepsilon - \delta) \mu_{22}^{HC} \frac{(C_4 + C_z^{min})}{K_6 + (C_4 + C_z^{min})} C_4$ Degradation of mesozooplankton in detritus (1.4)   | $\beta$          | Grazing efficiency coefficient   | –                      |
|   | $g_2^{max}$      | Maximal mesozooplankton ingestion rate                                   | day <sup>-1</sup>      |
|   | $\rho_{18}$      | Mesozooplankton grazing preference on microzooplankton                   | –                      |
|   | $Fac_2$          | Grazing preference normalization factor for mesozooplankton              | –                      |
| $\mu_{22}^{HC} = \mu_{21} + (\mu_{21}^{max} - \mu_{21}) (C_{11})^{mhc} + (K_6^{HC})^{mhc}$ Microzooplankton mortality rate from HC toxicity (1.5)   | $\varepsilon$    | Fractional micro- & mesozooplankton loss of ammonium                     | –                      |
|   | $\delta$         | Fractional micro- & mesozooplankton loss of LDON                         | –                      |
|   | $C_z^{min}$      | Minimal zooplankton concentration  | mmol N m <sup>-3</sup> |
|   | $K_6$            | Half saturation constant of micro- & mesozooplankton loss                | –                      |
| $\mu_{22}^{HC} = \mu_{21}^{HC}$ Mesozooplankton mortality rate from HC toxicity (1.6)   | $K_6^{HC}$       | Half saturation constant of micro- & mesozooplankton loss by HC toxicity | –                      |
|   | $mhc$            | Slope factor of micro- & mesozooplankton mortality for a sigmoid curve   | day <sup>-1</sup>      |
|   | $\mu_{21}^{max}$ | Maximal microzooplankton mortality rate                                  | day <sup>-1</sup>      |
|   | $\mu_{21}$       | Natural microzooplankton mortality rate                                  | day <sup>-1</sup>      |

2011; Reddy et al., 2012), establishing realistic HC consumption rates using C:N ratios was not possible. Thus, we chose concentrations within the 5–100  $\mu\text{L}^{-1}$  range (Almeda et al., 2013) and converted this equivalent to  $\text{mmol N m}^{-3}$  following a 1:1 HC to nitrogen ratio (see section on Chronic Oil Spill Scenario).

Consequently, the flux from the HC to the OHCB compartment (Figure 1) is the only biologically mediated loss of HC in the model that allows incorporation of HC into the biogeochemical pelagic environment (Table 1, Equation 1.1). The maximal HC uptake rate  $\nu b_2$  for this flux was chosen following Burchard et al. (2006). Here, we applied the same value as  $\nu b_1 = 1.2 \text{ day}^{-1}$ , representing maximal ammonium uptake by bacteria (BAC1).

Biodegradation also involves the consumption of nitrogen-based compounds. However, the form of nitrogen utilized by OHC bacteria in these processes is not known. Therefore, we hypothesized that the LDON compartment (Figure 1), which contains the most bioavailable form consumed by bacteria, applies a co-limitation on HC consumption. HC directly stimulates OHC bacterioplankton (BAC2), but they compete for substrate with BAC1, thus affecting the whole bacterioplankton super-compartment. Equation 1.2 in Table 1 describes the minimal HC to LDON uptake ratio for the OHCB compartment.

**Effects of HC on Zooplankton Mortality**  
Results from micro- and mesocosm experiments show different but directly noticeable effects of HC on the survival of zooplankton species. Finding that copepod species seemed to be strongly affected, Almeda et al. (2013) proposed a sigmoid numerical model of mortality with increasing HC concentration. Therefore, we integrated this relationship between mesozooplankton mortality and HC concentration with existing natural mortality rates  $\mu_{21}$  and  $\mu_{22}$  (Table 1, Equations 1.5 and 1.6). Because no specific mortality rates were available for microzooplankton species,

we applied the same HC toxicity to micro- and mesozooplankton (Table 1, Equations 1.3 and 1.4).

## CHRONIC OIL SPILL SCENARIO

Because chronic oil spills account for the majority of HC pollution in seawater (Potters, 2013), we chose to simulate a chronic oil spill that replicates an offshore oil leak. HC is incorporated into the system in a subsurface 5 m layer with a small time relaxation (seven days). In order to target the austral summer, the contamination period was set from August 1, 2013, to July 31, 2014. To evaluate different responses of the planktonic system to the contamination, we performed one control run at three levels of contamination (0, 10, 20, and 50  $\text{mmol N m}^{-3}$ ). Finally, each contamination level was run in the two physical configurations (stratified and well-mixed). For example,  $\text{CST}_{00}$  will be referenced as the control (00  $\text{mmol N m}^{-3}$ ) simulation in the STratified experiment using the latest Complete version of the biogeochemical model (Table S1).

## RESULTS

### Physical Environment Dynamics

In all simulations, wind stress shows a seasonal pattern, with the strongest average values during austral winter. However, in the stratified experiment, which aims to reproduce the stratified side of the tidal front in the southeastern region of the SJG, episodic wind events strongly influence upper layer mixing (Figures S2a and S3a) and result in deepening of biotic and abiotic variables at weekly timescales. In this same experiment, temperature shows a marked two-layer stratification pattern from November 2013 to April 2014 (Figure S2b). In the well-mixed experiment, temperature is almost vertically homogeneous, with maxima reaching 6.6°C and 15.8°C in September and March, respectively (Figure S3b). No vertical stratification is evident in either experiment (Figures S2c and S3c).

Horizontal currents are forced by external pressure gradients oscillating at the  $M_2$  tidal period. Maximum current

speeds occur in the upper 20 m of the water column and decrease toward the seafloor (Figure S3e) due to bottom friction (Figure S1).

### Distribution of HC

In the stratified experiment, vertical distribution of dissolved HC follows a summertime two-layer stratification close to the thermocline depth (Figure 2a–c). During winter, vertical mixing allows the deepening of low HC concentrations, which reach the bottom of the water column between August and October 2013. In the well-mixed experiment, almost vertically homogeneous concentrations can be observed from the beginning of the simulation for all levels of contamination with only subtle differences in the upper 30 m (Figure 2d–f).

In the stratified experiment, the lowest level of HC contamination ( $\text{CST}_{10}$ , Figure 2a), ranges from 1  $\text{mmol N m}^{-3}$  to 6  $\text{mmol N m}^{-3}$ , last measurable in surface waters at the end of September 2013. From the end of August to mid-October 2013, 2  $\text{mmol N m}^{-3}$  are found between 50 m and 80 m depth. By November 16, 2013, the system is clear of contamination. However, during the first week of May 2014, low concentrations between 0 m and 40 m appear again and last until the end of July that year. In the well-mixed experiment ( $\text{CWM}_{10}$ , Figure 2d), values range from 4  $\text{mmol N m}^{-3}$  to 5  $\text{mmol N m}^{-3}$  from late September to mid-October 2013. Thereafter, a quick reduction in concentrations is followed by the disappearance of HC two weeks earlier than in the stratified experiment.

At the highest level of contamination, contrasting results can be observed between the two experiments. In the stratified experiment ( $\text{CST}_{50}$ , Figure 2c), biodegradation processes never seem thoroughly effective throughout the simulation, and the maximal HC concentration at 32  $\text{mmol N m}^{-3}$  remains from early October to early December 2013 between 0 m and 20 m depth. Conversely, in the well-mixed experiment ( $\text{CWM}_{50}$ , Figure 2f), most of HC present is

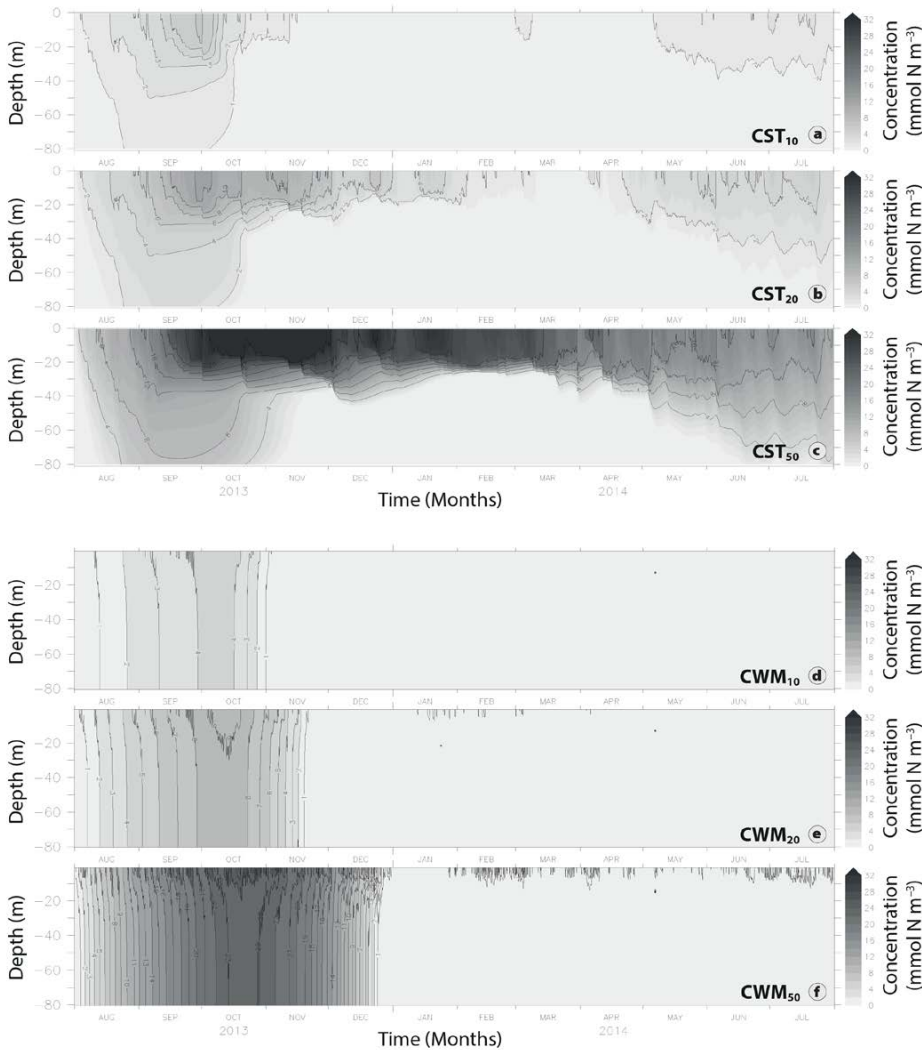


**FIGURE 2.** 2013/2014 annual cycle of HC concentration at 10 mmol N m<sup>-3</sup>, 20 mmol N m<sup>-3</sup>, and 50 mmol N m<sup>-3</sup> of contamination for the (a–c) stratified and the (d–f) well-mixed experiments, respectively.

degraded over the entire water column after five months. Moreover, maxima are significantly lower, with 24 mmol N m<sup>-3</sup> from the first week of October to the first week of November over the top 22 m of the water column.

### Effects of HC on Abiotic Compartments

In the control experiment CWM<sub>00</sub>, by mid-January 2014, 8 mmol N m<sup>-3</sup> of nitrate are still available, while this value is reached in late October 2013 in CWM<sub>20</sub>. In the stratified experiment, CST<sub>00</sub> and CST<sub>20</sub> results show concentrations reaching 12.5 mmol N m<sup>-3</sup> in the bottom layer (50 m to 80 m water depth) from mid-December 2013 to mid-May 2014. Between 0 m and 20 m,

minima between 0.5 mmol N m<sup>-3</sup> and 2 mmol N m<sup>-3</sup> are found from mid-December 2013 to the end of March 2014 for the CST<sub>00</sub> simulation, and from mid-October 2013 to the end of March 2014 for the CST<sub>20</sub> simulation.

In comparison to the CST<sub>00</sub> simulation, other simulation results show elevated concentrations of ammonium. CST<sub>10</sub>, CST<sub>20</sub>, and CST<sub>50</sub> present, respectively, values two, three, and seven times higher than the control CST<sub>00</sub> (Figure 3c). On April 13, the maximum reaches 15 mmol N m<sup>-3</sup> at 30 m depth for the CST<sub>20</sub> simulation (Figure 3d). These values can be explained by a sustained bacterial activity below the thermocline (Figure 4f). During the same period, vertical detritus dynamics (Figure S4d)

follow a similar pattern, confirming the active microbial loop in the HC contaminated experiments. In contrast, above the thermocline, lower concentrations, ranging from 2 mmol N m<sup>-3</sup> to 4 mmol N m<sup>-3</sup>, decrease to 0 mmol N m<sup>-3</sup> in December 2013 and January 2014. In the well-mixed experiment, vertical detritus distribution follows a very homogeneous pattern. Results from simulation CWM<sub>20</sub> show values seven times higher than the control in early June 2014.

LDON, as part of the biodegradation process, shows interesting variations, especially in the stratified experiment. In CST<sub>00</sub>, a slow depletion from 0.3 mmol N m<sup>-3</sup> in September 2013 to 0.05 mmol N m<sup>-3</sup> in May 2014 is evident between 0 m and 80 m depth (Figure 3a). In CST<sub>20</sub>, there is rapid depletion (from 0.30 mmol N m<sup>-3</sup> to 0.05 mmol N m<sup>-3</sup>) in the top 25 m of the water column from October 12, 2013, to the end of March 2014 (Figure 3b). This trend follows the presence of HC toward the beginning of winter 2014 (Figure 2c), diminishing until LDON is absent in the upper 60 m in June 2014. Furthermore, these concentrations do not show strong dependence on stratification.

### Effects of HC on Planktonic Compartments

The response of the phytoplankton, zooplankton, and bacterioplankton (BAC1) compartments to HC was studied. In Figures 4 and 5, we chose to compare results from simulations at 20 mmol N m<sup>-3</sup> of contamination to the control simulations.

In the stratified experiment, phytoplankton show very high concentrations at all levels of contamination. Results from the CST<sub>20</sub> simulation show maxima up to 8.7 times higher than the control values between 0 m and 30 m depth (Figure 4b). Moreover, the bloom periods shift from September (1.2 mmol N m<sup>-3</sup>) and December 2013 (1.5 mmol N m<sup>-3</sup>) for CST<sub>00</sub> to February (11.4 mmol N m<sup>-3</sup>) and March 2014 (13 mmol N m<sup>-3</sup>) for CST<sub>20</sub>. Figure 4d

shows that zooplankton are only present below the thermocline from November 2013 to June 2014 following the absence of HC (Figure 3b). Compared to the control, CST<sub>20</sub> displays concentrations of zooplankton two times higher during March and April 2014.

Concerning the bacterial super-compartment in CST<sub>20</sub>, BAC1 concentrations are only present below 30 m depth, with BAC2 predominating over the thermocline and reflecting effective biodegradation of HC from October 2013 to March 2014 (Figures 4f and S4d). Beneath the thermocline, the absence of HC in CST<sub>20</sub> makes it possible for zooplankton to grow and graze on sinking phytoplankton at the density interface from November 2013 to April 2014. However, from February 2014, microzooplankton that feed on bacterioplankton are dominant, supporting the hypothesis that there is strong BAC1 activity at 20 m to 45 m depth (Figure 4d,f).

In comparison, the well-mixed exper-

iment results show relatively homogeneous vertical distribution of each variable (Figure 5). Total bacterioplankton (Figure S5a), dominated by oil-degrading bacteria (80%) over the entire CWM<sub>20</sub> simulation, show concentrations (up to 24 mmol N m<sup>-3</sup>) in the same range as the CST<sub>20</sub> results values (up to 22 mmol N m<sup>-3</sup>; Figure S4). However, after December 2013, BAC1 increases up to four times the control concentrations (Figure 4f).

In early summer, concentrations of phytoplankton do not exceed 1.5 mmol N m<sup>-3</sup> and 4 mmol N m<sup>-3</sup> for the CWM<sub>00</sub> and CWM<sub>20</sub> simulations, respectively. However, in the CWM<sub>20</sub> simulation, rapid biodegradation (Figure 2e) lowers the concentrations of HC, reducing its impact on zooplankton (Figure 2e). Consequently, after the spring bloom period, zooplankton concentrations exceed 1.0 mmol N m<sup>-3</sup>, limiting phytoplankton growth to 2 mmol N m<sup>-3</sup> due to grazing pressure (Figure 5d).

### Temporal Changes in Plankton Size Classes

To illustrate temporal dynamics, phytoplankton and zooplankton concentrations resulting from the CST<sub>00</sub>, CST<sub>10</sub>, CST<sub>20</sub>, and CST<sub>50</sub> simulations were depth-integrated. In addition, because phytoplankton blooms are typically found in a two-layer structure in stratified experiments, we will concentrate on interpreting the stratified experiment only. Attention must be paid to the scale of Figure 6a, reduced from 290 mmol N m<sup>-2</sup> to 50 mmol N m<sup>-2</sup> for clarity.

In CST<sub>10</sub> (Figure 6b), the diatom bloom reaches five times the values found in the CST<sub>00</sub> simulation and persists until the end of November. Two diatom blooms occur during the third week of January 2014 and the third week of March 2014. Both are followed by mesozooplankton maxima. At this level of perturbation, zooplankton evolution is interesting. From the end of August 2013, microzooplankton concentration increases

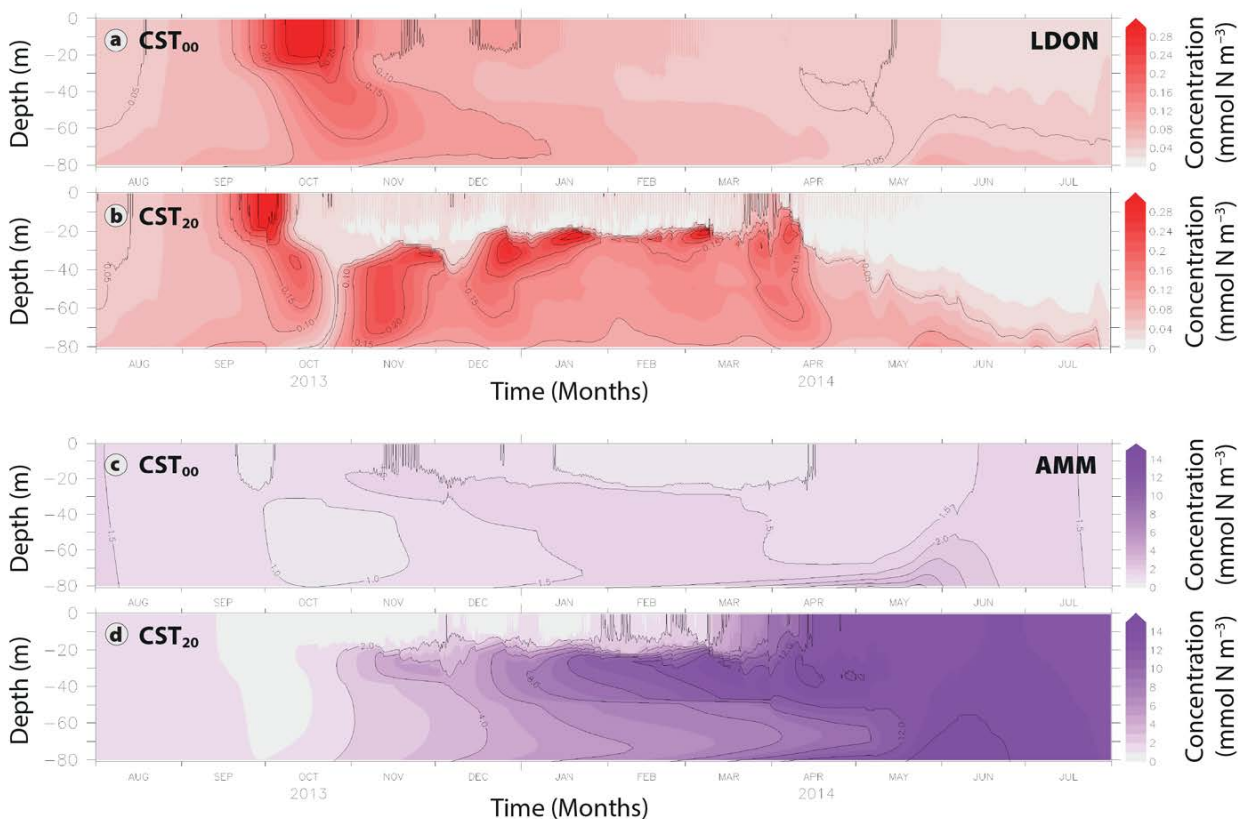
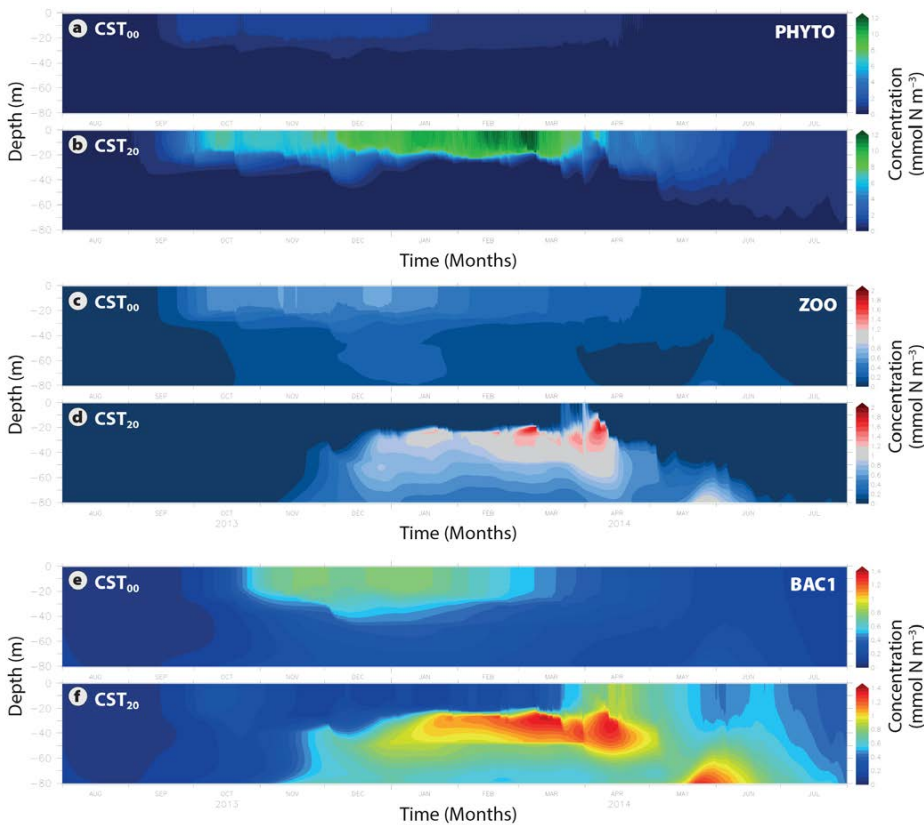
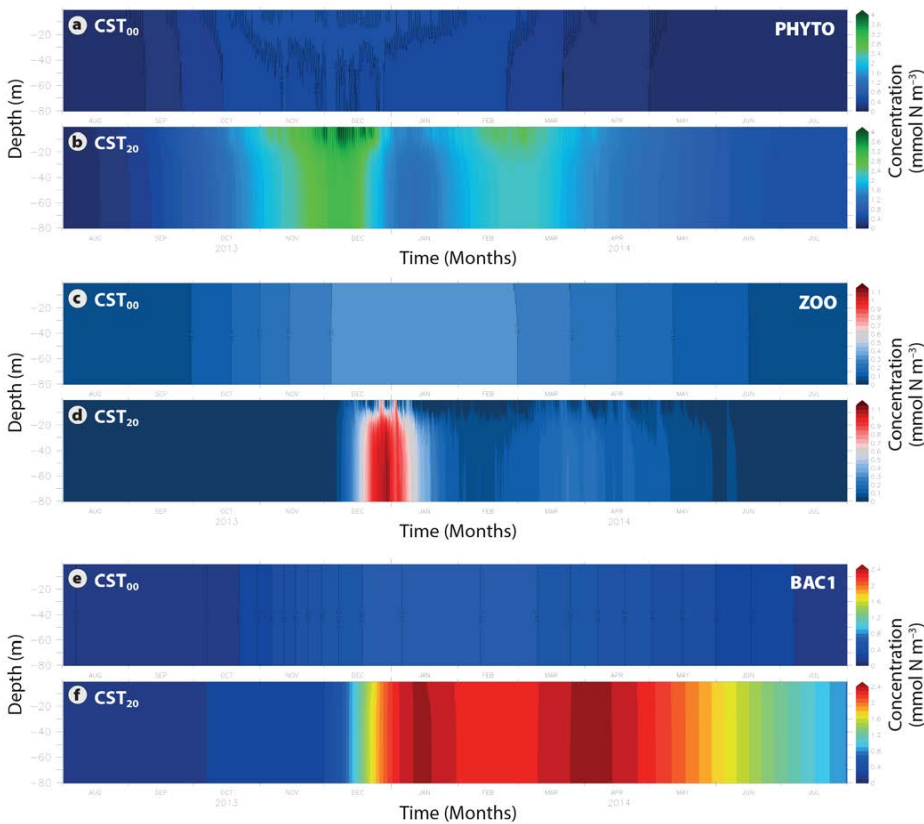


FIGURE 3. 2013/2014 annual cycle of simulated LDON from the (a) CST<sub>00</sub> and the (b) CST<sub>20</sub> simulations. Annual cycle in 2013/2014 of simulated ammonium (AMM) from the (c) CST<sub>00</sub> and the (d) CST<sub>20</sub> simulations.





**FIGURE 4.** 2013/2014 annual cycle of simulated phytoplankton (DIA+FLA) from (a) CST<sub>00</sub> and (b) CST<sub>20</sub> simulations, simulated zooplankton (MCZ+MSZ) from (c) CST<sub>00</sub> and (d) CST<sub>20</sub> simulations, and simulated bacteria (BAC1) from (e) CST<sub>00</sub> and (f) CST<sub>20</sub> simulations.



**FIGURE 5.** 2013/2014 annual cycle of simulated phytoplankton (DIA+FLA) from (a) CWM<sub>00</sub> and (b) CWM<sub>20</sub> simulations, simulated zooplankton (MCZ+MSZ) from (c) CWM<sub>00</sub> and (d) CWM<sub>20</sub> simulations, and simulated bacteria (BAC1) from (e) CWM<sub>00</sub> and (f) CWM<sub>20</sub> simulations.

despite the presence of HC. Results from CST<sub>20</sub> and CST<sub>50</sub> show diatoms are strongly dominant over the other groups. Micro- and mesozooplankton concentrations show similar increasing trends from the first week of November 2013 (Figure 6c,d).

## DISCUSSION

### Physical Environment

To understand the processes occurring within the plankton system during a chronic surface oil spill, we developed a one-dimensional coupled model that incorporates realistic physical conditions. Our results show that wind and tidally induced currents are the only contributors to the vertical mixing of biogeochemical variables in the SJG (Glorioso and Simpson, 1994; Glorioso and Flather, 1995; Palma et al., 2004). Temperature, the driving conservative property for stratification at the SJG latitude (Krepper and Rivas, 1979), is homogeneous during winter months. In the stratified experiment, a seasonal thermocline extended from spring to summer as previously described for the area by Akselman (1996). Moreover, satellite observations of sea surface temperature show similar values at the southeastern stratified region of the SJG (Glembocki et al., 2015).

In the well-mixed experiment, values of sea surface temperature are in accordance with Glembocki et al. (2015). Moreover, Carreto et al. (2007) show that vertically homogeneous conditions are also found in the southeastern SJG during spring and summer. The weak salinity variations are associated with the seasonal intrusion of the homogeneous low-salinity Magellan Plume at the south of the SJG (Krepper and Rivas, 1979; Palma and Matano, 2012). These homogeneous conditions agree with Palma et al. (2004), who point out that surface wind stress and strong tidally induced mixing due to bottom friction are the main external contributors to the vorticity balance in this region of the southwestern Atlantic shelf. Thus, in our model, HC distribution shows that contrasting turbulent regimes strongly affect

the distribution and dilution of the contaminant. In contrast, in the stratified experiment, higher HC concentrations are only found above the thermocline during spring and summer.

### Nutrients and Bacterioplankton Dynamics

In both experiments, nitrate depletion is associated with earlier phytoplankton development (nitrate consumption) in the presence of HC. However, studies conducted on the biogeochemistry of the Deepwater Horizon spill did not find correlations between nitrate concentrations and the presence of an HC plume (Shiller and Joung, 2012; Dubinsky et al., 2013). Increasing ammonium concentrations starting at the end of summer 2014 are not consistent with Shiller and Joung (2012), but Horel et al. (2014) showed that temperature and the amount of oil affect nitrogen cycling rates, and that results additionally depend on the time of the year of the spill.

When HC is present in the system, OHC bacteria become significant only after two to three months. At the beginning of the spill, biodegradation is limited by the low LDON concentrations found toward the end of winter. After the first phytoplankton bloom, detritus production is enhanced, fueling LDON bacterial activity. While detritus and LDON dynamics in the presence of HC have not previously been documented in the literature, it is crucial to mention that regulation of biodegradation is clearly not limited to one type of nutrient (Atlas and Bartha, 1972; Atlas, 1981; Shiller and Joung, 2012). Thus, understanding the preference and timing of nitrogen-based nutrient consumption remains challenging. Our results suggest that the physical regime, including turbulence, plays an important role in biodegradation efficiency during HC contamination (Hassanshahian and Cappello, 2013). In the stratified experiment, biodegradation removes most of the HC by the first week of February 2014. In comparison, the well-mixed experiment shows

faster incorporation of HC by OHC bacterioplankton, leading to the reduction of direct and indirect effects on plankton communities.

With HC altering bacterial dynamics, the higher concentrations of BAC1 beneath the thermocline in the simulation are associated with more intense detritus recycling and sinking. The shift that occurs in bacterial community structure in the upper water column in the CST<sub>20</sub> simulation is in accordance with the decline of bacterial diversity and the succession of Gammaproteobacteria that Hazen et al. (2010) and Dubinsky et al. (2013) observed following the Deepwater Horizon spill.

### Phytoplankton and Zooplankton

In the stratified experiment, HC indirectly affects phytoplankton, and concentrations reach values of up to 17 mg Chla m<sup>-3</sup>. These results are

consistent with those of Johansson (1978), who reports increasing phytoplankton biomass during the *Tsesis* oil spill in the Baltic Sea. This inordinately high-intensity phytoplankton growth is attributable not only to the absence of grazing pressure from zooplankton, which are absent from the upper water column, but also to the increasing ammonium concentrations toward summer.

Without HC in the system, diatoms are the dominant phytoplankton group, with a spring bloom occurring in late September, as previously reported in the study area (Akselman, 1996; Rivas et al., 2006). During the bloom peak, both micro- and mesozooplankton concentrations begin to increase in our model through herbivorous grazing, thus limiting diatom growth. Unfortunately, no field information is available on these groups to validate our results.

While our results show high diatom

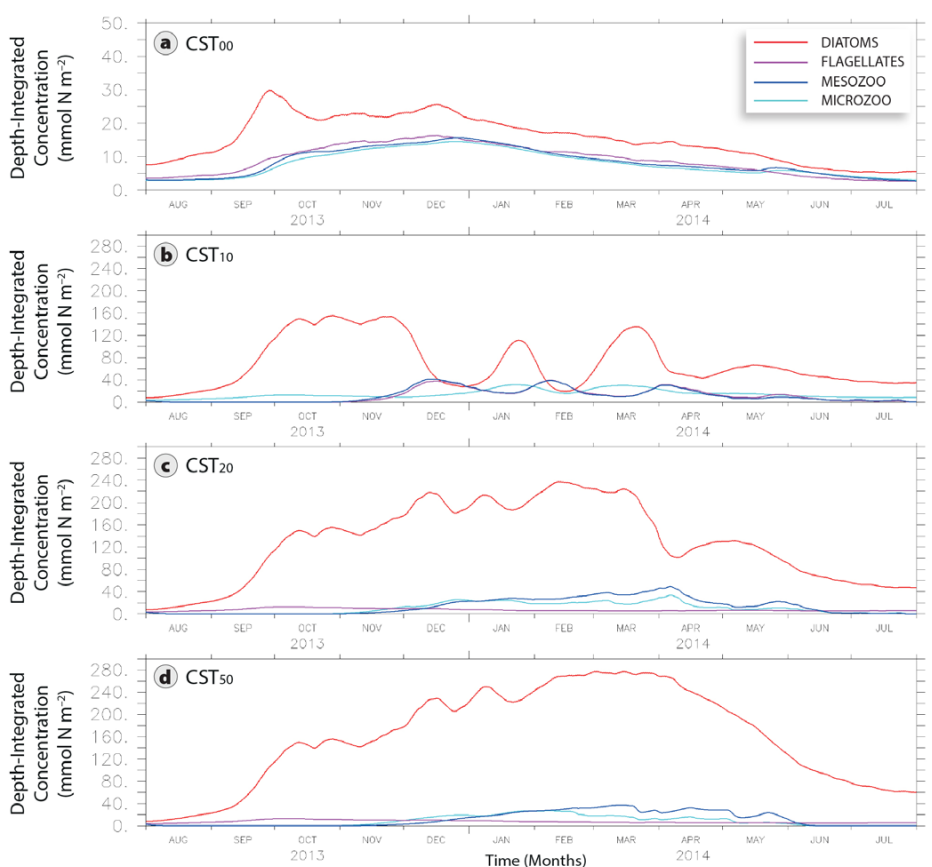


**FIGURE 6.** 2013/2014 annual cycle of simulated depth-integrated diatoms (red curve), flagellates (purple curve), microzooplankton (cyan curve), and mesozooplankton (blue curve) from (a) CST<sub>00</sub>, (b) CST<sub>10</sub>, (c) CST<sub>20</sub>, and (d) CST<sub>50</sub> simulations.

growth as an indirect consequence of HC contamination, results from other work are controversial: some studies show strong negative effects of HC contamination on this group (Hsiao, 1976; Siron et al., 1996; Nayar et al., 2005; Sargian et al., 2007), and others highlight its persistence in oil polluted environments (Gordon and Prouse, 1973; Johansson, 1978; Teal and Howarth, 1984). Here, we show that among the indirect effects, the decrease of zooplankton grazing leads to an increase in phytoplankton abundance, as suggested by Johansson (1978). Similarly, Baker (1971) and Cabioch et al. (1981) previously observed the increase in bacterial activity associated with the recycling of dead microorganisms. On the other hand, an increase of microzooplankton can be linked to grazing on bacterioplankton occurring in the lower part of the water column where HC concentrations are  $\leq 1 \text{ mmol N m}^{-3}$  (Figure 2a).

Previously discussed results indicate that the response of phytoplankton to HC contamination is species-specific. Further investigation is needed to carefully parameterize the direct effects of HC on phytoplankton.

## CONCLUSIONS

Modeling HC effects on a planktonic system requires consideration of several biogeochemical variables and processes. These model inputs result in a carbon flux imbalance in natural pelagic systems over an annual cycle. Our results suggest that in addition to the direct effects of HC on planktonic systems, indirect synergistic effects must also be considered.


The highly productive southeastern portion of the SJG shows different trends after subsurface incorporation of HC. In both experiments, at 10, 20, and 50  $\text{mmol N m}^{-3}$  of HC contamination, biodegradation of HC is limited during winter and starts at the beginning of spring only when primary production increases and, consequently, LDON concentrations are sufficiently high.

At 20  $\text{mmol N m}^{-3}$ , abnormally elevated concentrations of ammonium are

linked to strong recycling of detritus by bacteria (BAC1). In this case, the detritus compartment is fueled by dead zooplankton that are related to HC toxicity and strong phytoplankton exudation. Because nitrification is not taken into consideration, incorporation of HC into the planktonic system is reflected in the accumulation of nitrogen in the ammonium compartment.

The great dominance of diatoms over the other planktonic compartments is associated with the indirect effects (decrease of herbivorous grazing and increase of detritus formation).

Finally, the dynamically contrasting well-mixed region shows lower HC concentration over the entire water column, resulting in faster bacterial consumption. Nevertheless, zooplankton are less affected by contamination under these physical conditions. Here, turbulent mixing plays a key role in the rate of encounter between HC and the different biological variables.

In future work, key physical and biological parameterizations should help us refine the results presented in this study. Sensitivity analyses must be conducted to understand the importance of biodegradation rates and nutrient dependency on biodegradation. 

## SUPPLEMENTARY MATERIALS

Supplementary materials are available online at <https://doi.org/10.5670/oceanog.2018.413>.

## REFERENCES

- Acha, E.M., H.W. Mianzan, R.A. Guerrero, M. Favero, and J. Bava. 2004. Marine fronts at the continental shelves of austral South America: Physical and ecological processes. *Journal of Marine Systems* 44(1–2):83–105, <https://doi.org/10.1016/j.jmarsys.2003.09.005>.
- Akselman, R. 1996. Estudios Ecológicos en el Golfo San Jorge y Adyacencias (Atlántico Sudoccidental). Distribución, abundancia y variación estacional del fitoplancton en relación a factores físico-químicos y la dinámica hidrológica. Universidad de Buenos Aires. Tesis, 154 pp.
- Almeda, R., Z. Wambaugh, Z. Wang, C. Hyatt, Z. Liu, and E.J. Buskey. 2013. Interactions between zooplankton and crude oil: Toxic effects and bioaccumulation of polycyclic aromatic hydrocarbons. *PLoS ONE* 8(6):e67212, <https://doi.org/10.1371/journal.pone.0067212>.
- Anderson, J.W., J.M. Neff, B.A. Cox, H.E. Tatem, and G.M. Hightower. 1974. Characteristics of dispersions and water-soluble extracts of crude and

refined oils and their toxicity to estuarine crustaceans and fish. *Marine Biology* 27(1):75–88, <https://doi.org/10.1007/BF00394763>.

- Atlas, R.M. 1981. Microbial degradation of petroleum hydrocarbons: An environmental perspective. *Microbiology and Molecular Biology Reviews* 45(1):180–209.
- Atlas, R.M., and R. Bartha. 1972. Degradation and mineralization of petroleum in seawater: Limitation by nitrogen and phosphorous. *Biotechnology and Bioengineering* 14(3):309–318, <https://doi.org/10.1002/bit.260140304>.
- Baker, J.M. 1971. Seasonal effects of oil pollution on salt marsh vegetation. *Oikos* 22(1):106–110, <https://doi.org/10.2307/3543368>.
- Beazley, M.J., R.J. Martinez, S. Rajan, J. Powell, Y.M. Piceno, L.M. Tom, G.L. Andersen, T.C. Hazen, J.D. van Nostrand, J. Zhou, and others. 2012. Microbial community analysis of a coastal salt marsh affected by the Deepwater Horizon oil spill. *PLoS ONE* 7(7), <https://doi.org/10.1371/journal.pone.0041305>.
- Burchard, H., K. Bolding, W. Kühn, A. Meister, T. Neumann, and L. Umlauf. 2006. Description of a flexible and extendable physical–biogeochemical model system for the water column. *Journal of Marine Systems* 61(3–4):180–211, <https://doi.org/10.1016/j.jmarsys.2005.04.011>.
- Cabioch, L., J.C. Dauvin, F. Gentil, C. Retière, and V. Rivain. 1981. Perturbations induites dans la composition et le fonctionnement des peuplements benthiques sublittoraux, sous l'effet des hydrocarbures de l'Amoco Cadiz. Pp. 513–526 in *Amoco Cadiz, Fates and Effects of the Oil Spill*. CNEXO, Paris.
- Carreto, J.I., M.O. Carignan, N.G. Montoya, and A.D. Cucchi Colleoni. 2007. Ecología del fitoplancton en los sistemas frontales del Mar Argentino. Pp. 11–31 in *El Ecosistema Marino*. J.I. Carreto and C. Bremen, eds, INIDEP.
- Dubinsky, E.A., M.E. Conrad, R. Chakraborty, M. Bill, S.E. Borglin, J.T. Hollibaugh, O.U. Mason, Y.M. Piceno, F.C. Reid, W.T. Stringfellow, and others. 2013. Succession of hydrocarbon-degrading bacteria in the aftermath of the Deepwater Horizon oil spill in the Gulf of Mexico. *Environmental Science & Technology* 47(19):10,860–10,867, <https://doi.org/10.1021/es401676y>.
- Dunstan, W.M., L.P. Atkinson, and J. Natoli. 1975. Stimulation and inhibition of phytoplankton growth by low molecular weight hydrocarbons. *Marine Biology* 31(4):305–310, <https://doi.org/10.1007/BF00392087>.
- Fasham, M.J.R., H.W. Ducklow, and S.M. McKelvie. 1990. A nitrogen-based model of plankton dynamics in the oceanic mixed layer. *Journal of Marine Research* 48(3):591–639, <https://doi.org/10.1357/002224090784984678>.
- Fingas, M. 2016. *Oil Spill Science and Technology*. Gulf Professional Publishing, 1,078 pp.
- Flores-Melo, X., I.R. Schloss, C. Chavanne, G.O. Almandoz, M. Latorre, and G.A. Ferreyra. 2018. Phytoplankton ecology during a spring-neap tidal cycle in the southern tidal front of San Jorge Gulf, Patagonia. *Oceanography* 31(4):70–80, <https://doi.org/10.5670/oceanog.2018.412>.
- Gin, K.Y., M.K. Huda, W.K. Lim, and P. Tkalic. 2001. An oil spill-food chain interaction model for coastal waters. *Marine Pollution Bulletin* 42(7):590–597, [https://doi.org/10.1016/S0025-326X\(00\)00205-8](https://doi.org/10.1016/S0025-326X(00)00205-8).
- Glembocck, N.G., G.N. Williams, M.E. Góngora, D.A. Gagliardini, and J.M.L. Orensanz. 2015. Synoptic oceanography of San Jorge Gulf (Argentina): A template for Patagonian red shrimp (*Pleoticus muelleri*) spatial dynamics. *Journal of Sea Research* 95:22–35, <https://doi.org/10.1016/j.seares.2014.10.011>.

- Glorioso, P.D., and R.A. Flather. 1995. A barotropic model of the currents off SE South America. *Journal of Geophysical Research* 100(95):427–440. <https://doi.org/10.1029/95JC00942>.
- Glorioso, P.D., and R.A. Flather. 1997. The Patagonian Shelf tides. *Progress in Oceanography* 40(1–4):263–283. [https://doi.org/10.1016/S0079-6611\(98\)00004-4](https://doi.org/10.1016/S0079-6611(98)00004-4).
- Glorioso, P., and J. Simpson. 1994. Numerical modelling of the M2 tide on the northern Patagonian Shelf. *Continental Shelf Research* 14(2–3):267–278. [https://doi.org/10.1016/0278-4343\(94\)90016-7](https://doi.org/10.1016/0278-4343(94)90016-7).
- González, J., E. Fernández, F. Figueiras, and M. Varela. 2013. Subtle effects of the water soluble fraction of oil spills on natural phytoplankton assemblages enclosed in mesocosms. *Estuarine, Coastal and Shelf Science* 124:13–23. <https://doi.org/10.1016/j.ecss.2013.03.015>.
- Gordon, D.C., and N.J. Prouse. 1973. The effects of three oils on marine phytoplankton photosynthesis. *Marine Biology* 22(4):329–333. <https://doi.org/10.1007/BF00391389>.
- Hassanshahian, M., and S. Cappello. 2013. Crude oil biodegradation in the marine environments. Pp. 101–135 in *Biodegradation: Engineering and Technology*. R. Chamey, ed., Intech Open, <https://doi.org/10.5772/55554>.
- Hazen, T.C., E.A. Dubinsky, T.Z. DeSantis, G.L. Andersen, Y.M. Piceno, N. Singh, J.K. Jansson, A. Probst, S.E. Borglin, J.L. Fortney, and others. 2010. Deep-sea oil plume enriches indigenous oil-degrading bacteria. *Science* 330(6001):204–208. <https://doi.org/10.1126/science.1195979>.
- Horel, A., R.J. Bernard, and B. Mortazavi. 2014. Impact of crude oil exposure on nitrogen cycling in a previously impacted *Juncus roemerianus* salt marsh in the northern Gulf of Mexico. *Environmental Science and Pollution Research* 21(11):6,982–6,993. <https://doi.org/10.1007/s11356-014-2599-z>.
- Horowitz, A., and R.M. Atlas. 1977. Continuous open flow-through system as a model for oil degradation in the Arctic Ocean. *Applied and Environmental Microbiology* 33(3):647–653.
- Howarth, R.W. 1988. Nutrient limitation of net primary production in marine ecosystems. *Annual Review of Ecology and Systematics* 19:89–110. <https://doi.org/10.1146/annurev.es.19.110188.000513>.
- Hsiao, S.I.C. 1976. *Biological Productivity of the Southern Beaufort Sea: Phytoplankton and Seaweed Studies*. Fisheries and Marine Service, Environment Canada. Beaufort Sea Technical Report 12c, 99 pp.
- Hsiao, S.I.C., D.W. Kittle, and M.G. Foy. 1978. Effects of crude oils and the oil dispersant corexit on primary production of arctic marine phytoplankton and seaweed. *Environmental Pollution* 15(15):209–221. [https://doi.org/10.1016/0013-9327\(78\)90066-6](https://doi.org/10.1016/0013-9327(78)90066-6).
- Johansson, S. 1978. Impact of oil on the pelagic ecosystem. Pp. 61–80 in *The TESIS Oil Spill*. Report of the First Year Scientific Study (October 26, 1977 to December 1978).
- King, G., J. Kostka, T. Hazen, and P. Sobczyk. 2015. Microbial responses to the Deepwater Horizon oil spill: From coastal wetlands to the deep sea. *Annual Review of Marine Science* 7(1):377–401. <https://doi.org/10.1146/annurev-marine-010814-015543>.
- Krepper, C.M., and A.L. Rivas. 1979. Análisis de las características oceanográfica de la zona austral de la Plataforma Continental Argentina y aguas adyacentes. *Acta Oceanográfica Argentina* 2(2):55–82.
- Latorre, M.P., I.R. Schloss, G.O. Almandoz, K. Lemarchand, X. Flores-Melo, V. Massé-Beaulne, and G.A. Ferreyra. 2018. Mixing processes at the pycnocline and vertical nitrate supply: Consequences for the microbial food web in San Jorge Gulf, Argentina. *Oceanography* 31(4):50–59. <https://doi.org/10.5670/oceanog.2018.410>.
- Ministerio de Energía y Minería. 2016. Producción de petróleo en Argentina desde 1950. Tech. rep., Subsecretaría de Escenarios y Evaluación de Proyectos – Secretaría de Planificación Energética Estratégica. <https://datos.minem.gob.ar/dataset>.
- Musser, B.J., and P.K. Kilpatrick. 1998. Molecular characterization of wax isolated from a variety of crude oils. *Energy & Fuels* 12(4):715–725. <https://doi.org/10.1021/ef970206u>.
- Nayar, S., B.P.L. Goh, and L.M. Chou. 2005. Environmental impacts of diesel fuel on bacteria and phytoplankton in a tropical estuary assessed using in situ mesocosms. *Ecotoxicology* 14(3):397–412. <https://doi.org/10.1007/s10646-004-6373-8>.
- Palma, E.D., and R.P. Matano. 2012. A numerical study of the Magellan Plume. *Journal of Geophysical Research* 117(C5). <https://doi.org/10.1029/2011JC007750>.
- Palma, E.D., R.P. Matano, and A.R. Piola. 2004. A numerical study of the Southwestern Atlantic Shelf circulation: Barotropic response to tidal and wind forcing. *Journal of Geophysical Research* 109(C8). <https://doi.org/10.1029/2004JC002315>.
- Petroleum HPV Testing Group. 2011. *Crude Oil Category Assessment Document*. Technical Report, The American Petroleum Institute, 108 pp.
- Potters, G. 2013. *Marine Pollution*, 1st ed. Bookboon, 231 pp.
- Reddy, C.M., J.S. Arey, J.S. Seewald, S.P. Sylva, K.L. Lemkau, R.K. Nelson, C.A. Carmichael, C.P. McIntyre, J. Fenwick, G.T. Ventura, and others. 2012. Composition and fate of gas and oil released to the water column during the Deepwater Horizon oil spill. *Proceedings of the National Academy of Sciences of the United States of America* 109(50):20,229–20,234. <https://doi.org/10.1073/pnas.1101242108>.
- Reed, M., Ø. Johansen, P.J. Brandvik, P. Daling, A. Lewis, R. Fiocco, D. MacKay, and R. Prentki. 1999. Oil spill modeling towards the close of the 20<sup>th</sup> century: Overview of the state of the art. *Spill Science & Technology Bulletin* 5(1):3–16. [https://doi.org/10.1016/S1353-2561\(98\)00029-2](https://doi.org/10.1016/S1353-2561(98)00029-2).
- Rivas, A.L., A.I. Dogliotti, and D.A. Gagliardini. 2006. Seasonal variability in satellite-measured surface chlorophyll in the Patagonian Shelf. *Continental Shelf Research* 26(6):703–720. <https://doi.org/10.1016/j.csr.2006.01.013>.
- Sargian, P., S. Mas, É. Pelletier, and S. Demers. 2007. Multiple stressors on an Antarctic microplankton assemblage: Water soluble crude oil and enhanced UVBR level at Ushuaia (Argentina). *Polar Biology* 30(7):829–841. <https://doi.org/10.1007/s00300-006-0243-1>.
- Shiller, A.M., and D. Joung. 2012. Nutrient depletion as a proxy for microbial growth in Deepwater Horizon subsurface oil/gas plumes. *Environmental Research Letters* 7(4):045301. <https://doi.org/10.1088/1748-9326/7/4/045301>.
- Siron, R., E. Pelletier, and S. Roy. 1996. Effects of dispersed and adsorbed crude oil on microalgal and bacterial communities of cold seawater. *Ecotoxicology* 5(4):229–251. <https://doi.org/10.1007/BF00118994>.
- Teal, J.M., and R.W. Howarth. 1984. Oil spill studies: A review of ecological effects. *Environmental Management* 8(1):27–43. <https://doi.org/10.1007/BF01867871>.
- Valentine, D.L., I. Mezić, S. Maćešić, N. Črnjarić-Žic, S. Ivić, P.J. Hogan, V.A. Fonoberov, and S. Loire. 2012. Dynamic autoinoculation and the microbial ecology of a deep water hydrocarbon irruption. *Proceedings of the National Academy of Sciences of the United States of America* 109(50):20,286–20,291. <https://doi.org/10.1073/pnas.1108820109>.
- Yakimov, M.M., K.N. Timmis, and P.N. Golyshin. 2007. Obligate oil-degrading marine bacteria. *Current Opinion in Biotechnology* 18(3):257–66. <https://doi.org/10.1016/j.copbio.2007.04.006>.

## ACKNOWLEDGMENTS

We kindly acknowledge the contribution of the Ministerio de Ciencia, Tecnología e Innovación Productiva (MINCyT); the Provincia de Chubut; the Consejo Nacional de Investigaciones Científicas y Técnicas (CONICET) from Argentina, as well as the Institut des sciences de la mer de Rimouski-Université du Québec à Rimouski (ISMER-UQAR), and Québec Océan from Canada. Our thanks also to the captain and the crew of R/V *Coriolis II* during PROMESse.

## AUTHORS

**Philippe Klotz** (philippe.klotz@gmail.com) is a student at Institut des sciences de la mer de Rimouski (ISMER), Université du Québec à Rimouski, Québec, Canada. **Irene R. Schloss** is Researcher, Instituto Antártico Argentino, Centro Austral de Investigaciones Científicas, Tierra del Fuego, Argentina; Associate Professor, ISMER, Université du Québec à Rimouski, Québec, Canada; and Professor, Universidad Nacional de Tierra del Fuego, Ushuaia, Tierra del Fuego, Argentina. **Dany Dumont** is Professor, ISMER, Université du Québec à Rimouski, Québec, Canada.

## ARTICLE CITATION

Klotz, P., I.R. Schloss, and D. Dumont. 2018. Effects of a chronic oil spill on the planktonic system in San Jorge Gulf, Argentina: A one-vertical-dimension modeling approach. *Oceanography* 31(4):81–91. <https://doi.org/10.5670/oceanog.2018.413>.